nature photonics

LETTERS

PUBLISHED ONLINE: 6 JUNE 2010 | DOI: 10.1038/NPHOTON.2010.124

Coherent control of a single exciton qubit by optoelectronic manipulation

S. Michaelis de Vasconcellos[1]*†, S. Gordon[1], M. Bichler[2], T. Meier[1] and A. Zrenner[1]

The coherent state manipulation of single quantum systems is a fundamental requirement for the implementation of quantum information processors. Exciton qubits are of particular interest for coherent optoelectronic applications, in particular due to their excellent coupling to photons. Until now, coherent manipulations of exciton qubits in semiconductor quantum dots have been performed predominantly by pulsed laser fields. Coherent control of the population of excitonic states with a single laser pulse, observed by Rabi oscillations, has been demonstrated by several groups using different techniques[1–3]. By using two laser pulses, more general state control can be achieved[4], and coupling of two excitons has been reported[5,6]. Here, we present a conceptually new approach for implementing the coherent control of an exciton two-level system (qubit) by means of a time-dependent electric interaction. The new scheme makes use of an optical clock signal and a synchronous electric gate signal, which controls the coherent manipulation.

In this work, we make use of a two-level system, which is represented by the ground-state transition of a single exciton in a self-assembled InGaAs quantum dot (QD). For the experiment presented here, it is essential to have optical access to a single QD and electric field tunability of the ground-state transition. The QD is therefore embedded in the intrinsic region of an n–i Schottky diode, with optical access through a near-field shadow-mask (see Fig. 1a and Methods). The internal electric field in such structures can be controlled easily using an external bias voltage V_B. This provides a powerful way to accurately tune the energy of the two-level system by the quantum confined Stark effect. In the same regime, photocurrent (PC) spectroscopy can be applied as an efficient and quantitative method to determine the occupancy of the system. In the past, single-QD photodiodes as described above have been used in a variety of coherent experiments concerning the exciton ground state, including the demonstration of Rabi oscillations, Ramsey fringes, controlled rotation quantum gate operation, and most recently dressed states in a time-resolved fashion[7–12]. All those earlier experiments relied on the concept that resonant (or detuned) optical excitation from picosecond laser sources was used for coherent manipulations, and PC spectroscopy was used for detection.

In previous work, the bias voltage V_B was used only to statically control the energy of the two-level system. In contrast, we make use of fast voltage-induced qubit frequency control to implement coherent quantum phase manipulation. Implementation of the new electrically controlled manipulation scheme further requires resonant or nearly resonant optical double-pulse excitation, which is used as a stationary optical clock signal.

Throughout the paper we use the Bloch sphere representation as shown in Fig. 1b to display the quantum state of the two-level system. In this, the azimuthal angle reflects the quantum phase of the qubit, and the altitudinal-complement angle is related to the occupancy of the two-level system.

Coherent double-pulse excitation leads to the appearance of Ramsey fringes, which are typically controlled either in the time domain by the pulse delay time t_{delay} or in the frequency domain by energy tuning of the laser or the qubit[10]. In our experiment, Ramsey interference leads to a strong enhancement of the sensitivity of the coherent electric manipulation of the qubit, as explained in the following.

A first $\pi/2$ laser pulse creates a coherent superposition of both states if applied, for example, to a $|0\rangle$ state of the QD qubit. This

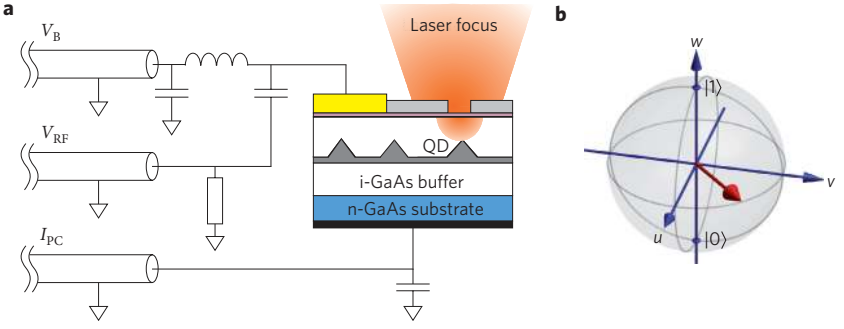

Figure 1 | Photodiode design and Bloch sphere. a, Schematic of a n–i-Schottky diode with electron-beam written shadow masks for optical access to single self-assembled InGaAs QDs. The single exciton ground-state transition is selected by resonant laser excitation. The attached electric circuitry allows for the supply of a d.c. bias voltage V_B and a 50 Ω terminated 2.4-GHz RF signal V_{RF}. The photocurrent I_{PC} is collected at the capacitively grounded back contact. **b**, Geometrical representation of the pure state of the two-level quantum system on the Bloch sphere by the Bloch vector (red). The *w*-axis represents the population, and the azimuthal angle of the Bloch vector in the *u*–*v*-plane represents the quantum phase of the two-level system.

[1]Universität Paderborn, Department Physik and Center for Optoelectronics and Photonics Paderborn (CeOPP), Warburger Str. 100, 33098 Paderborn, Germany, [2]Walter Schottky Institut, Technische Universität München, Am Coulombwall, 85748 Garching, Germany; †Present address: Laboratoire de Photonique et de Nanostructures, LPN/CNRS, Route de Nozay, 91460 Marcoussis, France. *e-mail: steffen.michaelis@lpn.cnrs.fr

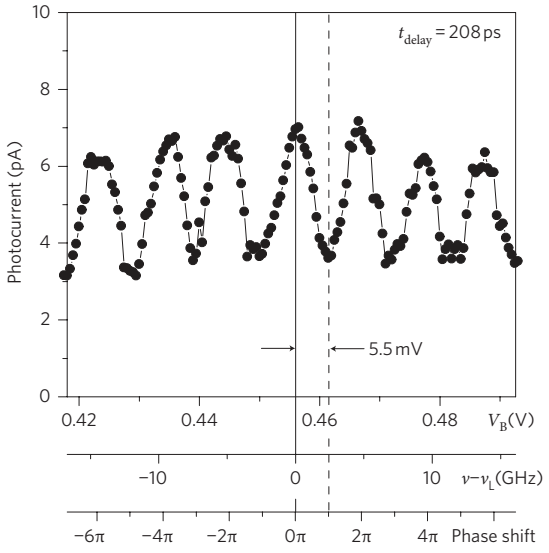

Figure 2 | Ramsey fringes. Photocurrent oscillations observed in a double-pulse experiment ($t_{delay} = 208$ ps) by tuning the energy of the quantum system by means of the bias voltage V_B (upper *x*-axis). The corresponding relative frequency shift from the resonance position (vertical solid line) is plotted on the middle axis. The lower axis denotes the relative phase shift between the quantum system and the light field. The vertical dashed line indicates the offset voltage required to achieve a phase shift of π.

coherent manipulation is also known as Hadamard gate. The quantum phase of the exciton qubit in this superposition is defined by the optical phase of the laser pulse, which is stored in the QD during the decoherence time. After a delay time, in which the phase of the system can evolve, the phase of the exciton qubit is probed by quantum interference with a second $\pi/2$ laser pulse. Depending on whether the two pulses are of the same or opposite optical phases, the superposition is turned into the $|1\rangle$ or $|0\rangle$ states, respectively. The result of such an experiment is the appearance of a PC oscillation as a function of static detuning by means of V_B. For the data shown in Fig. 2, t_{delay} was set to 208 ps, which is slightly less than the decoherence time for $V_B = 0.46$ V. For an increment in V_B of 5.5 mV, the quantum phase of the system is changed by π with respect to the optical phase. This corresponds to half a rotation of the Bloch vector around the equator of the Bloch sphere, and therefore to destructive interference (see Fig. 2). The sensitivity of the coherent electric manipulation in terms of ΔV_π scales like $1/t_{delay}$.

With the experiment presented in this paper we like to demonstrate coherent qubit manipulation by transient electric control for the condition of fixed optical excitation conditions. As shown in Fig. 3, the optical excitation (mode-locked Ti:sapphire laser) therefore comprises an optical clock signal, with consists of a stream of in-phase double pulses from a Michelson interferometer with constant delay ($t_{delay} = 208$ ps), pulse width ($t_{pulse} = 2.5$ ps) and pulse area ($2 \times \pi/2$). For the demonstration of the coherent optoelectronic control of the exciton qubit we further require an electric control signal, which can be applied synchronously with the optical clock. For the electric qubit manipulation, only the time interval between the picosecond pulse pair is effective. To create such a time-correlated electric signal, we generate the 30th harmonic of the laser repetition frequency (80 MHz), which is derived from the signal of a fast photoreceiver (see Fig. 3). We then obtain a 2.4-GHz radio frequency (RF) signal, which has a defined phase relation with respect to the laser pulses. By further electronic control we are able to sweep the phase φ and the amplitude V_{RF0} of this signal continuously, which means that the RF voltage can be adjusted according to $V_{RF}(t) = V_{RF0} \sin(\pi t/t_{delay} + \varphi)$.

The resulting signal is connected to the QD photodiode by superimposing it with the d.c. bias voltage V_B. To investigate the effect of the RF signal, we performed Ramsey-like experiments. It is important to note that the chosen time delay between the two laser pulses ($t_{delay} = 208$ ps) was set exactly to the half period time of the RF signal. This means, in particular, that we can continuously sweep between the situations in which either the upper or the lower half wave of the RF signal is lying exactly between the two laser pulses.

Coherent electric phase manipulation is based on the temporal detuning of the system within the delay time between the two laser pulses. The detuning is controlled by the applied coherent manipulation voltage $V_{CM}(t) = V_{RF}(t) + V_B - V_{res}$, which is the difference between the applied voltage $V_{RF}(t) + V_B$ and the voltage V_{res} at which the exciton qubit is in resonance with the light field.

To describe the optoelectronic phase control, it is convenient to define an electric pulse area A_{EL}, analogous to the optical pulse area,

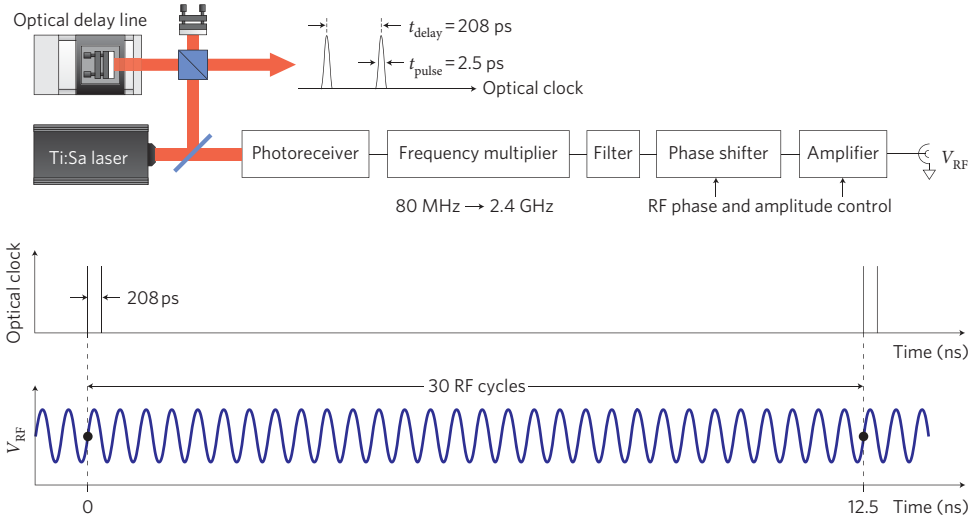

Figure 3 | Experimental set-up. A double-pulse optical clock signal ($t_{pulse} = 2.5$ ps, $t_{delay} = 208$ ps) is generated by a mode-locked Ti:sapphire laser (80 MHz repetition rate) followed by a Michelson interferometer. An 80-MHz sync signal from a fast photoreceiver is converted into the 30th harmonic at 2.4 GHz, which is time-correlated to the optical clock as shown in the timeline.

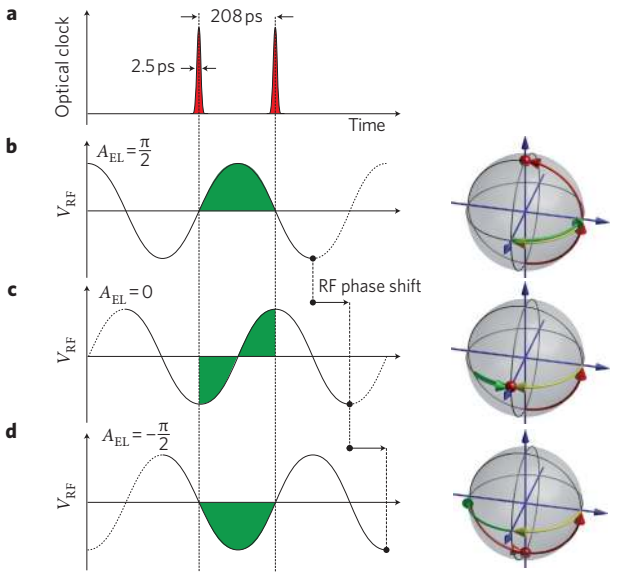

Figure 4 | Schematic representation of the electric phase manipulation. **a**, Optical clock on the timeline. **b–d**, Different optoelectronic manipulations as described in the text. On the Bloch spheres (right), the red and yellow arrows indicate the coherent optical manipulation and offset phase shift, respectively. The green arrows describe the coherent electric manipulation for different electric pulse areas A_{EL} as sketched on the left along the timeline. The final state of the quantum system after coherent operation is indicated by a red dot on each Bloch sphere.

which is well known from the theory of two-level systems[13]. The total phase shift induced by electric manipulation is given by

$$A_{EL} = \pi C_{CM} \int_0^{t_{delay}} V_{CM}(t)\mathrm{d}t \qquad (1)$$

where $V_{CM}(t)$ is responsible for the coherent manipulation and C_{CM} is the coherent electric manipulation coefficient (EMC). The unit of EMC is $[C_{CM}] = \mathrm{V}^{-1}\ \mathrm{s}^{-1}$; its magnitude is controlled by the steepness of the voltage-induced shift of the transition energy resulting from the Stark effect. The EMC can be obtained from voltage-controlled Ramsey experiments as the inverse product of t_{delay} and the necessary voltage shift to achieve a qubit phase shift of π. From the data shown in Fig. 2 we obtain $1/C_{CM} = 1.15 \pm 0.05$ V ps.

In Fig. 4 we present a detailed description of the experiment. The optical clock, consisting of two in-phase $\pi/2$ laser pulses, results in constructive quantum interference if the phase of the resonant quantum system remains unchanged. To achieve the highest possible qubit interference contrast between a RF-induced phase shift of $\pi/2$ and $-\pi/2$, we make use of a static offset voltage $V_{offset} = V_B - V_{res}$, which is chosen to be -2.75 mV, which leads to an additional phase shift of $-\pi/2$. This phase shift is illustrated on the Bloch sphere by a yellow arrow (Fig. 4). The same in-plane rotation of the Bloch vector could also have been obtained by introducing a $\pi/2$ phase shift between the two laser pulses.

For the situation shown in Fig. 4b, the positive half-wave of the RF signal is located between the two laser pulses. Hence, the quantum phase shift induced by V_{RF} is at a maximum. In the illustrated case, this corresponds to a RF-induced phase shift of $+\pi/2$, which is compensated by the offset phase shift to 0, leading to constructive quantum interference. For the second case (Fig. 4c), the RF-induced phase was changed to zero. Here, the Bloch vector is at first accelerated and then retarded, ending up at the starting point. No additional quantum phase shift is therefore created by the RF voltage. Owing to the action of V_{offset}, the total phase shift is $\pi/2$, and the second laser pulse leaves the exciton qubit in the superposition state. In the third case (Fig. 4d), the induced phase shift of $-\pi/2$ adds up with the action of V_{offset}, resulting in a total phase shift of π. The quantum interference is therefore destructive, rotating the Bloch vector to zero. For each of the three cases, the final state of the quantum system is indicated by a red circle on the Bloch spheres in Fig. 4.

In the experiment shown in Fig. 5a the electric phase is varied from 0 to 4π. For each electric phase setting, V_B was tuned from 0.42 to 0.47 V to obtain Ramsey fringes. In the resulting colour diagram we show colour-coded photocurrent data as a function of V_B and the RF phase. In the experiment we were able to adjust V_{RF0} in such a way that a sweep of the electric RF phase from 0 to π in fact results in an inversion of the observed Ramsey pattern. This inversion is related to an electrically induced quantum phase shift of nearly π. The observed oscillation amplitude is about a factor of two smaller compared to the conventional Ramsey experiment due to RF-induced heating. A detailed discussion of the heating is presented in the Supplementary Information.

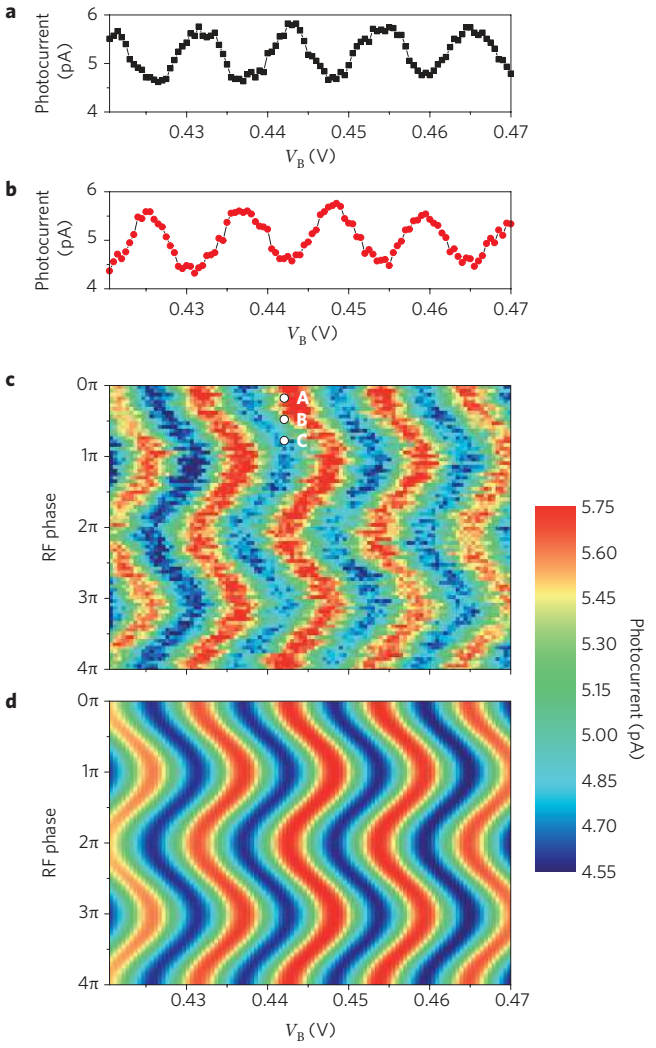

Figure 5 | Quantum phase shift. a,**b**, Photocurrent oscillations measured for a RF phase shift of 0 (**a**) and π (**b**). **c**, Coherent optoelectronic manipulations measured in photocurrent (colour coded). As indicated by points A, B and C, the phase of the quantum system can be inverted by electric manipulation by means of the RF phase. **d**, Corresponding theoretical model.

To quantitatively describe the experiment we consider a theoretical model based on optical Bloch equations and including the dephasing of the exciton due to tunnelling. The temporal detuning of the system due to the RF signal applied to the gate electrode is very small and relative slow compared to the overall dynamics of the quantum system. Thus we consider the temporal detuning as an adiabatic process. The only free fit parameters in this model are the amplitude and the absolute phase of the RF. Owing to the influence of parasitic contributions to the RF impedance of the photodiode (bond wire, internal capacitance), the exact magnitude of V_{RF} on the gate electrode remains unknown. A simulation of the resulting PC response was performed by solving these extended optical Bloch equations with a fourth-order Runge–Kutta algorithm. By comparing the result of the calculations (Fig. 5b) with the experimental data (Fig. 5a), we find that our model can reproduce the experiment with high accuracy. The best agreement is found for an applied RF amplitude of $V_{RF0} = 4.4 \pm 0.1$ mV, which corresponds to $1/C_{CM} = 1.17 \pm 0.03$ V ps. This is consistent with the EMC obtained from conventional Ramsey experiments ($1/C_{CM} = 1.15 \pm 0.05$ V ps) described before.

In conclusion we have described and experimentally demonstrated a new scheme for the coherent optoelectronic manipulation of an exciton qubit in a QD. With our contribution we have shown that it is possible to manipulate an optically clocked quantum system in the coherent regime only by applying a specific electric gate signal. This approach combines state-of-the-art picosecond laser techniques with synchronous electronics operating in the coherent regime of quantum systems.

Methods

Experiment. The sample was grown by molecular beam epitaxy on a (100)-oriented n^+-GaAs substrate. The QDs were embedded in a 360-nm-thick intrinsic GaAs layer, 40 nm above the n-doped GaAs back contact of the photodiode. The Schottky contact on top of the sample was formed from a semi-transparent titanium layer. The areal density of the InGaAs QDs was low enough to address a single QD through a near-field shadow mask. A detailed description of the sample structure is given in ref. 14.

The resonant optical clock ($\lambda = 926.7$ nm) was delivered by a 2.5-ps pulsed Ti:sapphire laser, with a repetition frequency of $f = 80$ MHz followed by a Michelson interferometer to create the double pulse. The interferometer consists of a coarse positioner with an attached nano-positioner stage to control the time delay and optical phase between the two laser pulses. The laser beam was focused on the shadow mask of the sample with a microscope objective (NA = 0.75) in a cryogenic set-up ($T = 4.2$ K).

The conversion of the 80-MHz sync signal from the laser to the 2.4-GHz RF signal was performed by standard RF components (see Fig. 3). As shown in Fig. 1a, V_{RF} was terminated (50 Ω) and capacitively coupled to the gate electrode of the photodiode by a RF network, which was placed close to the sample at the low-temperature stage.

Simulation. To simulate the QD system we first included the exciton tunnelling as a two-step relaxation process characterized by fast electron tunnelling and slow heavy-hole tunnelling[15]. The fast electron tunnelling rate and an additional pure dephasing term then determined the total dephasing time of the quantum system. The corresponding voltage-dependent time constants for the electron and heavy-hole tunnelling were obtained from previous experiments[16], and the electric tuning characteristics of the quantum system was derived from Stark effect measurements in the relevant bias voltage range. A detailed description of the theoretical model is presented in the Supplementary Information.

Received 23 October 2009; accepted 16 April 2010; published online 6 June 2010

References

1. Stievater, T. H. *et al.* Rabi oscillations of excitons in single quantum dots. *Phys. Rev. Lett.* **83,** 133603 (2001).
2. Kamada, H., Gotoh, H., Temmyo, J., Takagahara, T. & Ando, H. Exciton Rabi oscillation in a single quantum dot. *Phys. Rev. Lett.* **87,** 246401 (2001).
3. Borri, P. *et al.* Rabi oscillations in the excitonic ground-state transition of InGaAs quantum dots. *Phys. Rev. B* **66,** 081306 (2002).
4. Bonadeo, N. H. *et al.* Coherent optical control of the quantum state of a single quantum dot. *Science* **282,** 1473–1476 (1998).
5. Li, X. *et al.* An all-optical quantum gate in a semiconductor quantum dot. *Science* **301,** 809–811 (2003).
6. Unold, T., Mueller, K., Lienau, C., Elsaesser, T. & Wieck, A. Optical control of excitons in a pair of quantum dots coupled by the dipole–dipole interaction. *Phys. Rev. Lett.* **94,** 137404 (2005).
7. Zrenner, A., Beham, E., Stufler, S. & Findeis, F. Coherent properties of a two-level system based on a quantum-dot photodiode. *Nature* **418,** 612–614 (2002).
8. Takagi, H., Nakaoka, T., Watanabe, K., Kumagai, N. & Arakawa, Y. Coherently driven semiconductor quantum dot at a telecommunication wavelength. *Opt. Express* **16,** 013949 (2008).
9. Stufler, S. *et al.* Two-photon Rabi oscillations in a single $In_xGa_{1-x}As$/GaAs quantum dot. *Phys. Rev. B* **73,** 125304 (2006).
10. Stufler, S., Ester, P., Zrenner, A. & Bichler, M. Ramsey fringes in an electric-field-tunable quantum dot system. *Phys. Rev. Lett.* **96,** 037402 (2006).
11. Boyle, S. J. *et al.* Two-qubit conditional quantum-logic operation in a single self-assembled quantum dot. *Phys. Rev. B* **78,** 075301 (2008).
12. Boyle, S., Ramsay, A., Fox, A. & Skolnick, M. Beating of exciton-dressed states in a single semiconductor InGaAs/GaAs quantum dot. *Phys. Rev. Lett.* **102,** 207401 (2009).
13. Allen, L. & Eberly, J. H. *Optical Resonance and Two Level Atoms* (Wiley, 1975).
14. Zrenner, A. *et al.* Recent developments in single dot coherent devices. *Phys. Status Solidi (b)* **243,** 3696–3708 (2006).
15. Kolodka, R. S. *et al.* Inversion recovery of single quantum-dot exciton based qubit. *Phys. Rev. B* **75,** 193306 (2007).
16. Stufler, S., Ester, P., Zrenner, A. & Bichler, M. Quantum optical properties of a single $In_xGa_{1-x}As$–GaAs quantum dot two-level system. *Phys. Rev. B* **72,** 121301 (2005).

Acknowledgements

The authors acknowledge financial support from the German Federal Ministry of Education and Research (BMBF) through grant no. 01BM466 and from the German Research Foundation (DFG) research training group (no. GRK 1464).

Author contributions

S.M.d.V. and A.Z. conceived and designed the concept and experiment. M.B. fabricated the sample. S.M.d.V. and S.G. performed the experiments. S.M.d.V., S.G. and T.M. developed the theoretical model. S.M.d.V., T.M. and A.Z. analysed the data and wrote the paper.

Additional information

The authors declare no competing financial interests. Supplementary information accompanies this paper at www.nature.com/naturephotonics. Reprints and permission information is available online at http://npg.nature.com/reprintsandpermissions/. Correspondence and requests for materials should be addressed to S.M.d.V.